Ecological Modelling 481 (2023) 110325

Contents lists available at ScienceDirect

Ecological Modelling

journal homepage: www.elsevier.com/locate/ecolmodel

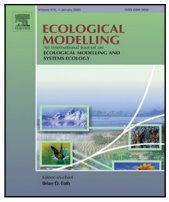

Modeling food dependent symbiosis in *Exaiptasia pallida*

Jakob O. Kaare-Rasmussen *, Holly V. Moeller, Ferdinand Pfab

Department of Ecology, Evolution and Marine Biology, University of California, Santa Barbara, 93106, CA, USA

ARTICLE INFO

Dataset link: https://doi.org/10.5281/zenodo.7699157

Keywords:
DEB model
Mutualism
Parasitism
Anemone
Cnidaria
Symbiodiniaceae
Endosymbiosis

ABSTRACT

Cnidaria, marine invertebrates that include reef-building stony corals, often rely on photosynthetic endosymbionts to obtain the energy they need for growth. Increased temperatures and/or nutrient pollution can disrupt mutualistic properties of the symbiosis, leading to host mortality. However, the precise mechanism by which this dysbiosis occurs is still unclear. Sea anemones, other cnidarians that may host algal endosymbionts, are used as a model organism for the coral holobiont to understand the costs and benefits of symbionts, but the exact nature of the costs of symbionts on the hosts is still unclear. Here we developed a Dynamic Energy Budget (DEB) model and fit the model to data from the anemone *Exaiptasia pallida* and its endosymbiotic algae, *Breviolum minutum*, in order to identify the most likely mechanism of symbiont costs. In order to match the laboratory dataset, our model needed an explicit symbiont demand term, in which the symbiont can "consume" host tissue to forcibly extract nitrogen. The model demonstrates the role of the symbiont as an amplifier of the host's state: a growing anemone grows better with symbionts, while a malnourished anemone looses biomass faster with a symbiont than without. This model allows us to project Cnidaria holobiont growth as a function of environmental conditions and adds a new framework for which to capture the direct cost a symbiont has on Cnidaria hosts.

1. Introduction

Coral reefs are among the most productive ecosystems on the planet (Crossland et al., 1991; Fisher et al., 2015). This biodiversity is supported by a symbiotic relationship that stony corals (and some other Cnidaria) share with photosynthetic dinoflagellates in the family Symbiodiniaceae. Cnidarian hosts obtain photosynthate from their algal endosymbionts in exchange for nitrogen. This increases nutrient recycling efficacy and supports coral growth in nutrient-poor environments (Muscatine and Porter, 1977). However, the close relationship between Cnidaria and their algal symbionts can break down under thermal stress resulting in the symbionts being expelled from the Cnidaria tissue, a phenomenon referred to as coral bleaching (Van Oppen and Lough, 2018). As climate change increases the frequency and severity of coral bleaching, it is important to understand this mutualism between Cnidarians and their symbionts, especially conditions in which this mutualism degrades and potentially becomes parasitic (Hughes et al., 2018).

To understand the balance of mutualism and parasitism in Cnidarian-dinoflagellate symbioses, we need to understand the translocation of nutrients between the host and symbiont. It is well known that Cnidarian hosts share nitrogen and other nutrients with their symbionts, while symbionts share carbohydrates with their hosts (Clayton and Lasker, 1984; Farrant et al., 1987; Muscatine and Cernichiari, 1969). The exact mechanism of translocation of nutrient between host and symbiont is still not fully understood. One supported mechanism for the translocation of nutrients from symbiont to host is that the host releases a "host release factor" (HRF) that encourages the symbiont to share photosynthate with the host rather than storing the photosynthate for its own use (Davy and Cook, 2001; Grant et al., 2006; Davy et al., 2012). A potential way to approximate this dynamic is by assuming that the symbiont uses some photosynthetically acquired carbon for growth, and shares the remaining carbon with the host. The host only receives leftover carbon from photosynthesis.

Reverse translocation of nutrients from the host to the symbiont is significantly less well understood (Davy et al., 2012). The symbiont receives phosphate and nitrogen in the form of ammonium (NH_4^+) (Davy et al., 2012). The symbiont may also receive carbon from the host, (Cook, 1972; Davy et al., 2012) though reverse translocation of carbon is thought to be minor in comparison to the products of photosynthesis, especially in well-lit environments (Falkowski and Raven, 2013; Davy et al., 2012; Cornwall, 2017). Though symbionts hosted by *Acropora* corals may acquire and use carbon from the host, it is suggested that symbionts in the anemone *Exaiptasia pallida* do not (Jinkerson et al., 2022). Furthermore, some isolated *Symbiodinium*

* Corresponding author.
E-mail address: jkaare-rasmussen@ucsb.edu (J.O. Kaare-Rasmussen).

https://doi.org/10.1016/j.ecolmodel.2023.110325
Received 17 July 2022; Received in revised form 8 February 2023; Accepted 17 February 2023
Available online 17 March 2023

have been shown to be capable of feeding (Jeong et al., 2012), and there are many examples of *Symbiodinium* heterotrophically acquiring nutrients from a host (Baker et al., 2018; Steen, 1987; Tremblay et al., 2016; Steen, 1988). Indeed, some *Symbiodinium* have been shown to impose significant and potentially fatal heterotrophic burdens on the host (Siegel, 1960; Steen, 1986; Peng et al., 2020). The shift from mutualism to parasitism of *Symbiodinium* under different environments has been reported in excavating sponges (Fang et al., 2017), in jellyfish (Sachs and Wilcox, 2006), and in the gastropod *Strombus gigas* (Banaszak et al., 2013).

To understand the shift from mutualism to parasitism in corals, scientists often use the sea anemone *E. pallida* as a model system. *E. pallida* shares many characteristics with corals, but it is easy to maintain in the laboratory and can survive with or without symbionts. This allows for studies that vary conditions for inoculated and aposymbiotic anemones to understand the impacts the symbionts have on the anemone. Peng et al. (2020) studied the impact that food deprivation stress has on the mutualism–parasitism balance found in *E. pallida*. They grew anemones inoculated with the endosymbiotic alga *Brevolium minutum* and aposymbiotic anemones under fed and starved conditions, and measured the changes in the symbiotic and anemone population over 8 weeks. This study showed a surprising amplification effect of symbionts on anemone performance: While well-fed anemones grew faster with symbionts than without them, starved anemones shrank and died much faster when they were inoculated with symbionts. This amplifying effect shows the important role the environmental conditions have on the balance between mutualism and parasitism.

There are a few existing models that describe the transfer of nutrients between the host and the symbiont in Cnidarian-dinoflagellate systems (Muller et al., 2009; Cunning et al., 2017; Xu et al., 2022). These models do not directly capture the significant cost a symbiont can incur on a host which is evident in the starved anemone in the experiments by Peng et al. (2020) and other examples of symbiont parasitism in cnidarian-dinoflagellate systems (Stat et al., 2008; Wooldridge, 2010). To close this gap, we constructed a Dynamic Energy Budget (DEB) model of the interactions between an anemone host and its symbiotic algae, including mechanisms through which the symbiont not only shares carbon with the host but also inflicts a metabolic burden. DEB models describe the rate of nutrient assimilation and utilization of organisms as a function of their environments (van der Meer, 2006; Nisbet et al., 2000; Kooijman, 2001). Simplified DEB models and theory have previously been used to describe nutrients exchange between a tree's roots and a tree's shoots (Russo et al., 2022). Similarly, our DEB model describes the nutrient exchange between *E. pallida* and *B. minutum*as seen in the experiments of Peng et al. (2020). We built this model based on the assumption that the host only receives leftover carbon, and we approximated reverse translocation and the metabolic cost of the symbiont on the host as the symbiont consumes the host. We tested the ability of this approximation to capture the amplification effect found by Peng et al. (2020). We parameterized the model with the 6 data sets provided by Peng et al. (2020) to validate the model. Once validated, we perturbed the model to simulate variations in environmental conditions and original parameters to extend the model predictions.

2. Methods

2.1. Model description

To understand how resource translocation explains the symbiont amplification effect seen in Peng et al. (2020), we developed a bioenergetic model that focuses on the nitrogen and carbon dynamics of the system. To describe this system, we considered two state variables: host biomass (H) and symbiont biomass (S). We focused on nitrogen and carbohydrates as the nutrients that mediate the relationship between the host and its symbionts. A diagram of this system is shown in Fig. 1. The parameters used to describe this system are listed in Table 2 and state variables and fluxes are in Table 1 . We used two Ordinary Differential Equations (ODEs) to describe the rate of change of the host biomass (H) and the symbiont biomass (S) over time:

$$\frac{dS}{dt} = j_{sg} - j_{st} \tag{1}$$

$$\frac{dH}{dt} = j_{hg} - j_{ht} \tag{2}$$

Here j_{sg} is the symbiont growth rate, j_{st} is the symbiont turnover rate, j_{hg} is the host growth rate and j_{ht} is the host turnover rate. Turnover rate is the rate at which biomass is lost, including natural mortality. The change in symbiont biomass over time is described as the difference between total symbiont growth rate and symbiont turnover rate. Similarly, the rate of change of the host biomass is described as the difference between total host growth rate and total host turnover rate.

The growth of the symbiont is dependent on how much nitrogen and carbon the symbiont has at any given time. The total symbiont growth rate is described as

$$j_{sg} = min(j_{sc}, n_{sn}^{-1} j_{sn}) \tag{3}$$

where j_{sc} is the total flux of carbon to the symbiont and j_{sn} is the total flux of nitrogen to the symbiont. The parameter n_{sn} is the nitrogen to carbon ratio of the symbiont. We used n_{sn} to adjust moles nitrogen to moles carbon needed for symbiont growth. The symbiont follows Liebig's law of the minimum, and grows at a rate determined by the stoichiometrically limiting nutrient (von Liebig, 1841).

The total symbiont turnover rate j_{st} is described as

$$j_{st} = d_s\, S \tag{4}$$

where d_s is the per-symbiont death rate.

In this model, the symbiont only acquires nitrogen through consuming the host, so j_{sn} is the total symbiont consumption of the host $f(S, H)$,

$$j_{sn} = y_n\, n_{hn}\, f(S, H) \tag{5}$$

adjusted by the conversion efficiency of host nitrogen to symbiont nitrogen, y_n. Furthermore, the function $f(S, H)$ describes the total consumption of the host by the symbionts in units of carbon moles. Therefore, the nitrogen to carbon ratio of the host, n_{hn}, is used to adjust moles of host carbon to moles of host nitrogen.

The symbiont can acquire carbon from photosynthesis at rate p and from consuming the host,

$$j_{sc} = p\, S \tag{6}$$

In *E. pallida* the symbionts do not receive carbon or cannot grow only using host carbon (Jinkerson et al., 2022).

The host growth (j_{hg}) also follows Liebig's law of the minimum, and grows at a rate determined by the stoichiometrically limiting nutrient (von Liebig, 1841). The total host growth rate is described as

$$j_{hg} = min(j_{hc}, n_{hn}^{-1} j_{hn}) \tag{7}$$

where j_{hc} is the flux of carbon to the host and j_{hn} is the flux of nitrogen to the host. Since the host biomass is measured in carbon moles, the flux of nitrogen, j_{hn}, is converted to carbon moles with the parameter n_{hn}. The parameter n_{hn} is the nitrogen to carbon ratio of the host.

The turnover of the host is dependent on the base mortality of the host, d_h, and the mortality caused by the symbiont consuming the host, $f(S, H)$:

$$j_{ht} = f(S, H) + d_h\, H \tag{8}$$

The host can only acquire nitrogen through feeding, which we assume is proportional to the hosts surface. The nitrogen uptake rate of the host is thus

$$j_{hn} = r_n\, H^{2/3} \tag{9}$$

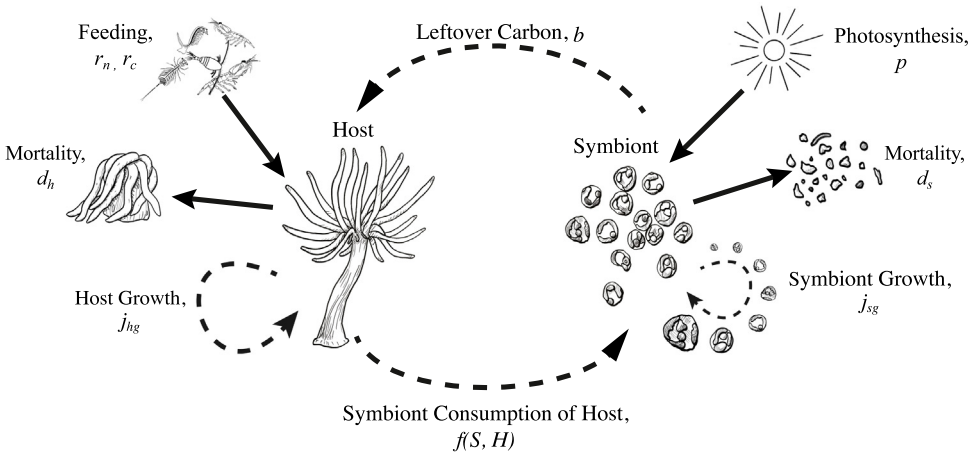

Fig. 1. Model diagram of anemone biomass (H) and symbiont biomass (S). All solid lines are fixed rates, while dotted lines are rates that depend on other aspects of the model. The anemone have a nitrogen uptake rate r_n and a carbon uptake rate r_c. The host can also acquire carbon from the symbiont at rate b, where b is the leftover carbon from the symbiont. The host's growth rate (j_{hg}) is dependent on the amount of carbon and nitrogen available to the host at any given time. The host also has a mortality rate of d_h. The symbiont can acquire carbon through photosynthesis at rate p. The symbiont also consumes the host as described by $f(S, H)$, providing the symbiont with nitrogen. The symbiont also has a growth rate (j_{sg}) which is dependent on the amount of carbon and nitrogen available to the symbiont at any given time. Lastly, the symbiont also has its own mortality rate, d_s. Illustrations by Elise Cypher.

where $H^{2/3}$ is proportional to the surface of the host and r_n is the surface specific nitrogen uptake rate of the host.

The host can acquire carbon both through leftover carbon from the symbiont at rate b and from surface specific uptake at rate r_c:

$$j_{hc} = b + r_c\ H^{2/3} \tag{10}$$

where $H^{2/3}$ is proportional to the surface of the host. Furthermore, we assumed that the host only receive the leftover photosynthate that the symbiont would otherwise be allocating to long term storage (Davy and Cook, 2001; Grant et al., 2006; Davy et al., 2012). Therefore, the translocation of carbon from the symbiont to the host b is defined as:

$$b = j_{sc} - j_{sg} \tag{11}$$

The function b is the total amount of carbon fixed by the symbiont minus the amount of carbon the symbiont uses for its own growth.

We will use a Holling Type II functional response of the per symbiont consumption of the host ($\frac{H}{S}$) to approximate the total metabolic cost of the symbiont on the host, and the translocation of nutrients from the host to the symbiont. The Holling Type II functional response is characterized as a decelerating rate of consumption of prey by the predator as prey density increases, eventually reaching an asymptote (Holling, 1959). Here we classify the symbiont as the predator consuming the host, which is interpreted as the prey. The function

$$f(S, H) = S\frac{a\frac{H}{S}}{1 + aw\frac{H}{S}} \tag{12}$$

$$= S\frac{aH}{S + awH} \tag{13}$$

describes the total consumption of the host by the symbiont in the system. The parameter a is the attack rate of the symbiont on the host, which is the initial slope of the functional response. The parameter w is the symbiont handling time, the average time for a unit of symbiont to handle a unit of host.

Putting together all parts of the model, the full equations are:

$$\frac{dS}{dt} = Min[pS, \frac{aHn_{hn}Sy_n}{Sn_{sn} + aHn_{sn}w}] - d_sS \tag{14}$$

$$\frac{dH}{dt} = -\frac{aHS}{S + aHw} - d_hH + Min[\frac{H^{2/3}r_n}{n_{hn}}, H^{2/3}r_c + pS - Min[pS, \frac{aHn_{hn}Sy_n}{Sn_{sn} + aHn_{sn}w}]] \tag{15}$$

We parameterized this model with the data from Peng et al. (2020). In order to use the data provided by Peng et al. (2020), we first converted from units of anemone base area mm^2 and number of symbiont cells to mol C of host (H) and mol C of symbiont (S). Our method for biomass conversion is shown in Appendix A. We used a log-likelihood approach to optimize the model fit for the Peng et al. (2020) data. Our parameter fitting method is described in Appendix B. To quantify the uncertainty of the parameter values, we used the Bias-Corrected and Accelerated (BC_a) bootstrapping method, which is shown in Appendix C. All model fitting and model analysis was doen in Mathematica 13.2 (Wolfram Research, Inc., 2021).

3. Results

3.1. The model reproduces observed anemone-symbiont dynamics

Our model both qualitatively and quantitatively captures anemone and algal dynamics observed by Peng et al. (2020) (Fig. 2). The model captures the increase in anemone biomass under fed conditions and the decrease in the anemone biomass under starved conditions. The model also captures the two different symbiont dynamics found in the inoculated treatments.

While the model fits the data well, there are some small differences between the model predictions and the data. Particularly, the symbiont biomass in the starved treatment did not peak at the same magnitude as the data (Fig. 2E). Furthermore, the model predicts a constant decline of the host biomass in the starved inoculated treatment, rather than a period of no change in the first four weeks followed by a quick decline as seen in the data (Fig. 2C). It is unclear why starved anemones, with symbionts, do not lose biomass immediately in the Peng et al. (2020) study. It may be that the host is still digesting food that was eaten before the start of the experiment, and using carbon from the symbiont, to maintain the same biomass before the host runs out of undigested food and begins to lose biomass. Despite some differences in the data, and the model predictions, the model captures the key dynamics of the system. We also explored the equilibrium dynamics of the model and found that a fed host with symbiont has a much higher equilibrium biomass than a fed host without symbiont (Figure S1). Furthermore, the symbiont is predominantly nitrogen limited regardless of initial biomass of the host and symbiont at the fitted parameter values, while the host shifts from carbon limited to nitrogen limited as the symbiont biomass increases (Figure S2).

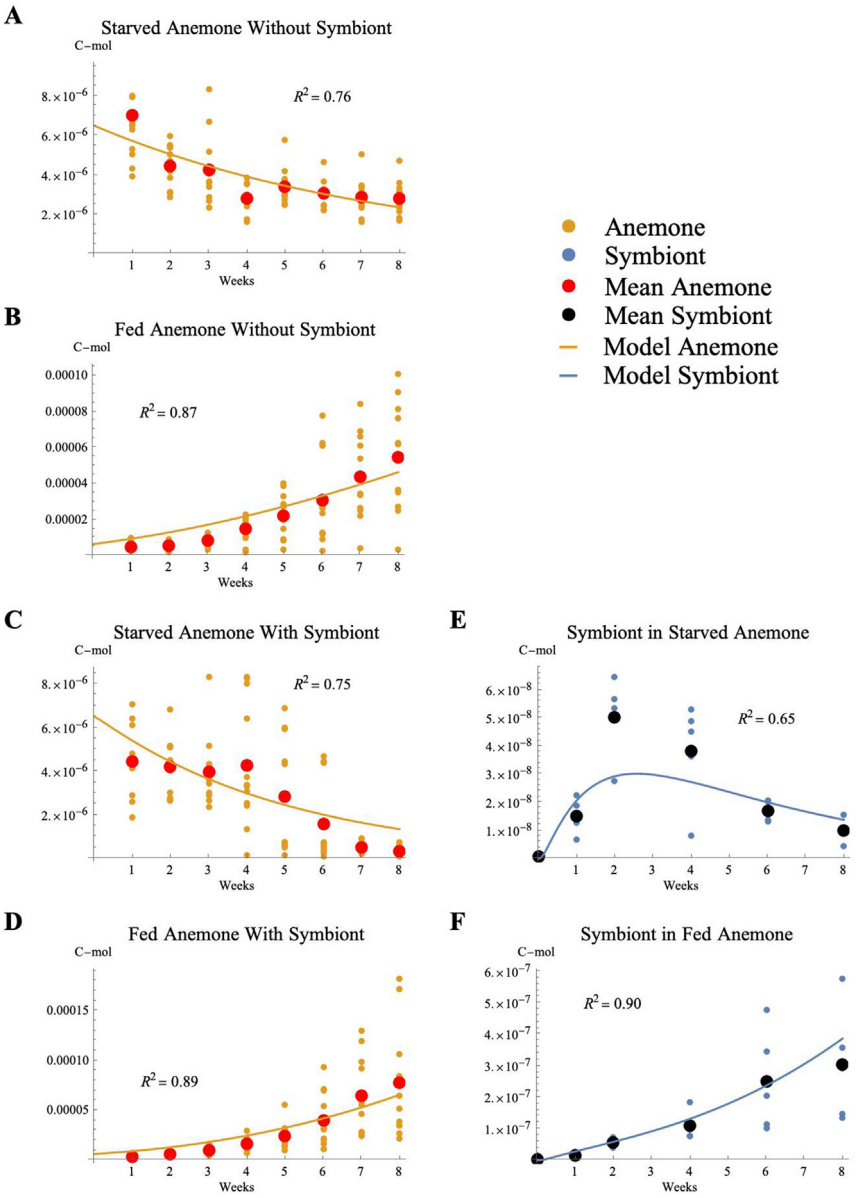

Fig. 2. Model predictions and data from Peng et al. (2020) for anemone and symbiont biomass of fed and starved anemone when inoculated and aposymbiotic. Each row represents a separate treatment. The model parameter values were fitted to the all 6 data sets from the Peng et al. (2020) study. All parameters remain the same through all four treatments, except initial symbiont biomass was set to zero in aposymbiotic treatments, and the host carbon and nitrogen uptake rates were set to zero in the starved treatments. Fitted parameter values are shown in Table 2. For each treatment, we calculated an R^2 value to compare the model fit to the experimental data.

Table 1
Model state variables and fluxes.

Variable	Description	Unit	Equation number
S	Symbiont biomass	mol C	–
H	Host biomass	mol C	–
j_{sg}	Symbiont growth rate	mol C week^{-1}	(3)
j_{st}	Symbiont turnover rate	mol C week^{-1}	(4)
j_{hg}	Host growth rate	mol C week^{-1}	(7)
j_{ht}	Host turnover rate	mol C week^{-1}	(8)
j_{hc}	Flux of carbon to Host	mol C week^{-1}	(10)
j_{sc}	Flux of carbon to Symbiont	mol C week −1	(6)
j_{hn}	Flux of nitrogen to Host	mol N week^{-1}	(9)
j_{sn}	Flux of nitrogen to Symbiont	mol N week^{-1}	(5)
b	Leftover carbon shared with host	mol C week^{-1}	(11)

Table 2
Model variables and parameters.

Variable	Description	Unit	Parameter estimate[a]
a	Symbiont attack rate	week^{-1}	0.0724 (0.0409, 0.108)
w	Symbiont handling time	week	0.00261 (0.00165, 0.00446)
p	Photosynthesis rate	week^{-1}	27.7 (11.7, 50.2)
r_c	Host carbon uptake rate (Fed Treatments)	week^{-1}	0.00999 (0.00904, 0.0109)
r_n	Host nitrogen uptake rate (Fed Treatments)	mol N mol C^{-1} week^{-1}	0.0146 (0.00265, 0.00446)
r_c	Host carbon uptake rate (Starved Treatments)	week^{-1}	0
r_n	Host nitrogen uptake rate (Starved Treatments)	mol N mol C^{-1} week^{-1}	0
y_n	Host nitrogen to symbiont nitrogen conversion efficiency of nitrogen	mol N mol N^{-1}	0.0602 (0.0295, 0.101)
n_{hn}	Nitrogen to carbon ratio of Host	mol N mol C^{-1}	0.18[b]
n_{sn}	Nitrogen to carbon ratio of Symbiont	mol N mol C^{-1}	0.13[‡]
d_s	Symbiont mortality rate	week^{-1}	0.771 (0.514, 1.25)
d_h	Host mortality rate	week^{-1}	0.126 (0.105, 0.156)
S_0	Initial Symbiont biomass	mol C	$1.02 \cdot 10^{-10}$ ($1.00 \cdot 10^{-10}$, $1.03 \cdot 10^{-10}$)
H_0	Initial Host biomass	mol C	$6.50 \cdot 10^{-6}$ ($5.86 \cdot 10^{-6}$, $7.41 \cdot 10^{-6}$)

[a]Optimal parameter; (95% CI).
[b]Parameter values from Cunning et al. (2017).

3.2. Mutualism and Parasitism Balance in varied environmental conditions and parameter values

A vital component of this system, as described by, Peng et al. (2020) is the switch from mutualism in fed anemone to parasitism in starved anemone. To quantify the effect of the symbiont on the host, we define δ as a measure of the magnitude of mutualism or parasitism in the system at a given set of parameters. We calculate δ as the difference between the model predictions of inoculated host biomass (H_i) and the model prediction of aposymbiotic host biomass (H_a) at a given set of parameter values:

$$\delta = H_i - H_a \tag{16}$$

We compute δ after 8 weeks of simulation, following the 8 week experiment duration used by Peng et al. (2020). For $\delta < 0$ the relationship is parasitic, as the symbiont decreases the host's biomass over time (starved anemone; Fig. 3A). For $\delta > 0$ the relationship is mutualistic, as the symbiont increases the host's biomass over time (fed anemone; Fig. 3B).

We plotted δ as a function of one parameter at a time, while holding all other parameter values constant at their fitted parameter values (Fig. 4). The most dominant trend shown throughout these figures is that when the host is carbon limited, and the symbiont provides more carbon to the host than the cost of hosting a symbiont, then $\delta > 0$ and the system is mutualistic. When the host is nitrogen limited or the carbon cost of hosting a symbiont outbalances the carbon shared from the symbiont, then $\delta < 0$, and the system is parasitic. (See Figure S3 for exploration of how nutrient limitation produces the dynamics observed in Fig. 4.) Particularly:

- varying attack rate, a, initially increases δ as the symbiont has more access to nitrogen, but once the cost of a hight attack rate begins to outweigh the benefit, δ decreases below zero.
- increasing handling time, w, decreases δ as the symbiont gains less nitrogen from the host
- varying photosynthesis rate, p, initially decreases δ as the symbiont can survive and are costly to the host, but do not share carbon. Further increasing p results in more carbon shared to the host and δ increases.
- varying host to symbion nitrogen conversion efficiency, y_n, initially decreases δ as the symbiont can survive, but does not share significant carbon. Further, increasing y_n results in more carbon shared with the host and δ increases.
- increasing symbiont mortality rate, d_s, decreases δ as this parameter makes the symbiont lose biomass and thus becomes less beneficial
- increasing host mortality rate, d_h, decreases δ as the host dies quickly regardless of the symbiont
- increasing host carbon uptake rate, r_c, initially increases δ as the symbiont supplements the host's carbon, but once the host becomes nitrogen-limited, and acquires all the needed carbon on its own, the symbiont is just a cost.
- initial increases in the host nitrogen uptake rate, r_n decreases δ. Extra nitrogen helps the host maintain biomass at the beginning of the experiment but also allows significant symbiont population growth, leading to an overshoot of symbiont where the host biomass collapses rapidly. Further, increasing r_n inverts the trend leading to an increase in δ as the extra nitrogen allows the host to sustain a beneficial symbiont population. Simulations of this mechanism are shown in figure S7 in the Supplementary Materials.

We further investigated the effect of two environmental factors known to strongly impact Cnidarian systems: nutrient availability and light conditions (Falkowski et al., 1984; Morris et al., 2019) (Fig. 5).

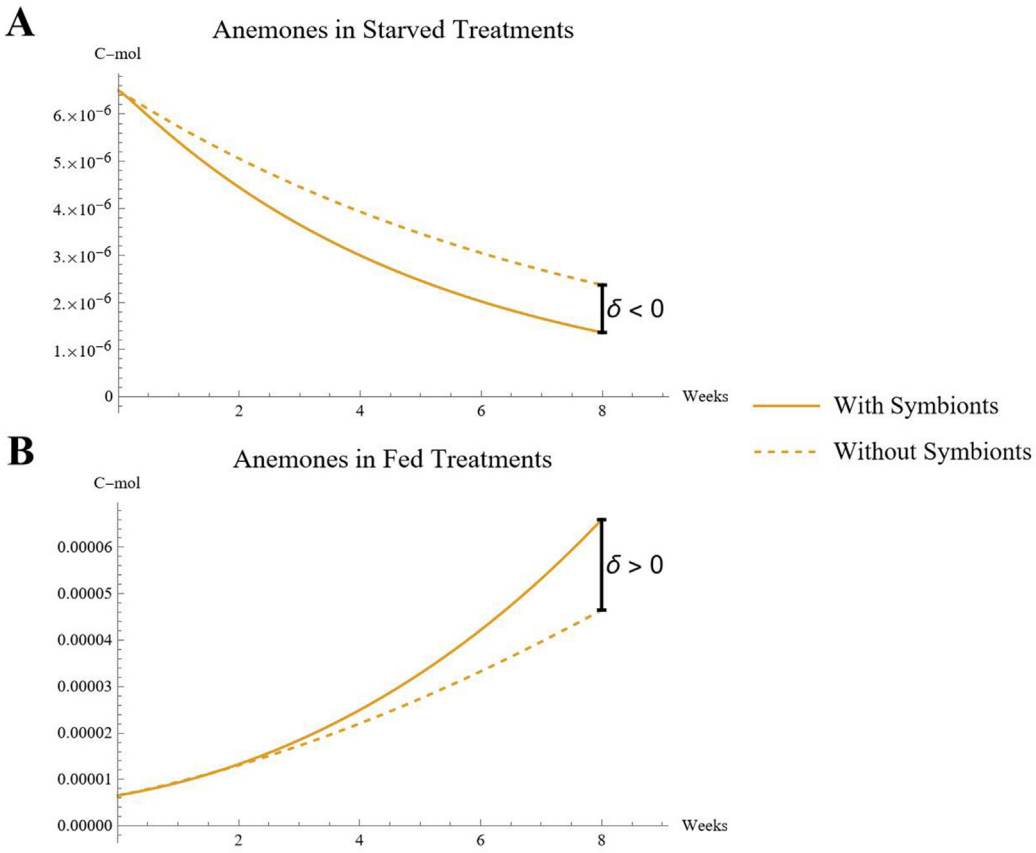

Fig. 3. Model prediction at fitted parameter values for fed and starved anemones when inoculated and aposymbiotic. The amplification effect of the symbiont, as described by Peng et al. (2020) is captured by this model with the fitted parameter values. The metric δ is the difference between the biomass of an inoculated anemone and an aposymbiotic anemone after 8 weeks. The symbiont is deemed mutualistic when $\delta > 0$ and parasitic when $\delta < 0$.

We jointly varied nutrient availability and light condition to explore the combined impacts on the symbiont–host symbiosis. We approximated nutrient availability with a combined host uptake rate R, which determines host carbon uptake rate as $r_c = R$ and host nitrogen uptake as $r_n = \gamma R$. Hereby γ is the ratio of nitrogen uptake rate to carbon uptake rate of the fitted parameter values, $\gamma = \frac{r_n}{r_c} = 1.466$. Further, we approximated changes in the light availability by directly altering the photosynthetic rate p. The system is predominant parasitic at low photosynthesis rates, and predominantly mutualistic at higher photosynthesis rate (Fig. 5A). Changes in photosynthesis have similar impacts on δ regardless of combined uptake rate, though the effect of increasing p is amplified at higher uptake rates (Fig. 5B). At low photosynthesis rates, there is little to no carbon shared from the symbiont to the host, so the cost of hosting a symbiont is greater than the benefit and $\delta < 0$ (Fig. 5C). At a high photosynthesis rate, the symbiont has leftover carbohydrates, and shares a lot with the host, increasing the benefit to the host. Conversely, increases in uptake rate increase parasitism at low photosynthesis rates but increase mutualism at higher photosynthesis rates. Figures S4, S5, and S6 in the supplementary material further explore the nutrient limitations leading to the dynamics seen in Fig. 5.

4. Discussion

Though Cnidarian-Dinoflagellate symbioses are often considered mutualisms, the role of endosymbiotic algae exists on a continuum between mutualism and parasitism (Stat et al., 2008; Wooldridge, 2010). Changes in environmental conditions can shift the role of symbionts from mutualism to parasitism (Baker et al., 2018). Our simple bioenergetics model highlights how symbionts can be environmental amplifiers, increasing the magnitude of host responses to the environment. Our findings recapitulate Peng et al. (2020). Our validated model demonstrates the importance of nutrient limitations to the balance of parasitism and mutualism. It is clear that symbionts are only beneficial to the anemone host in this model when the anemone is both carbon limited, and receives more carbon than it looses to the added metabolic cost of hosting a symbiont. Conversely, the symbionts are predominantly controlled by the availability of nitrogen both in this model, and experimentally (Xiang et al., 2020). Improving one characteristic of the system may not result in higher magnitude of mutualism. As feeding rates of the host, or food availability, increase, the symbionts are only beneficial to the host if there is a sufficiently high photosynthesis rate.

Though the costs of symbionts on Cnidarian hosts are well reported (Lesser et al., 2013; Peng et al., 2020; Steen, 1986), the exact mechanisms are still unclear. Similarly, the apparent importance of the reverse translocation of nitrogen in this system is still unclear (Rädecker et al., 2018; Davy et al., 2012). The model presented here approximates these uncertainties through one combined approximation of the symbiont consuming the host. This allows the symbiont to impose a metabolic cost on the host, and to acquire nitrogen (and potentially carbon) from the interaction. Further, this approximation recapitulates the balance between mutualism and parasitism found in the Peng et al. (2020) study.

There are a few limitations of this approximation. This model simplifies the ability for symbionts to get nitrogen and simplifies the expulsion of symbionts from an anemone host. In our model, the symbiont can only acquire nitrogen directly from consuming the host. In reality,

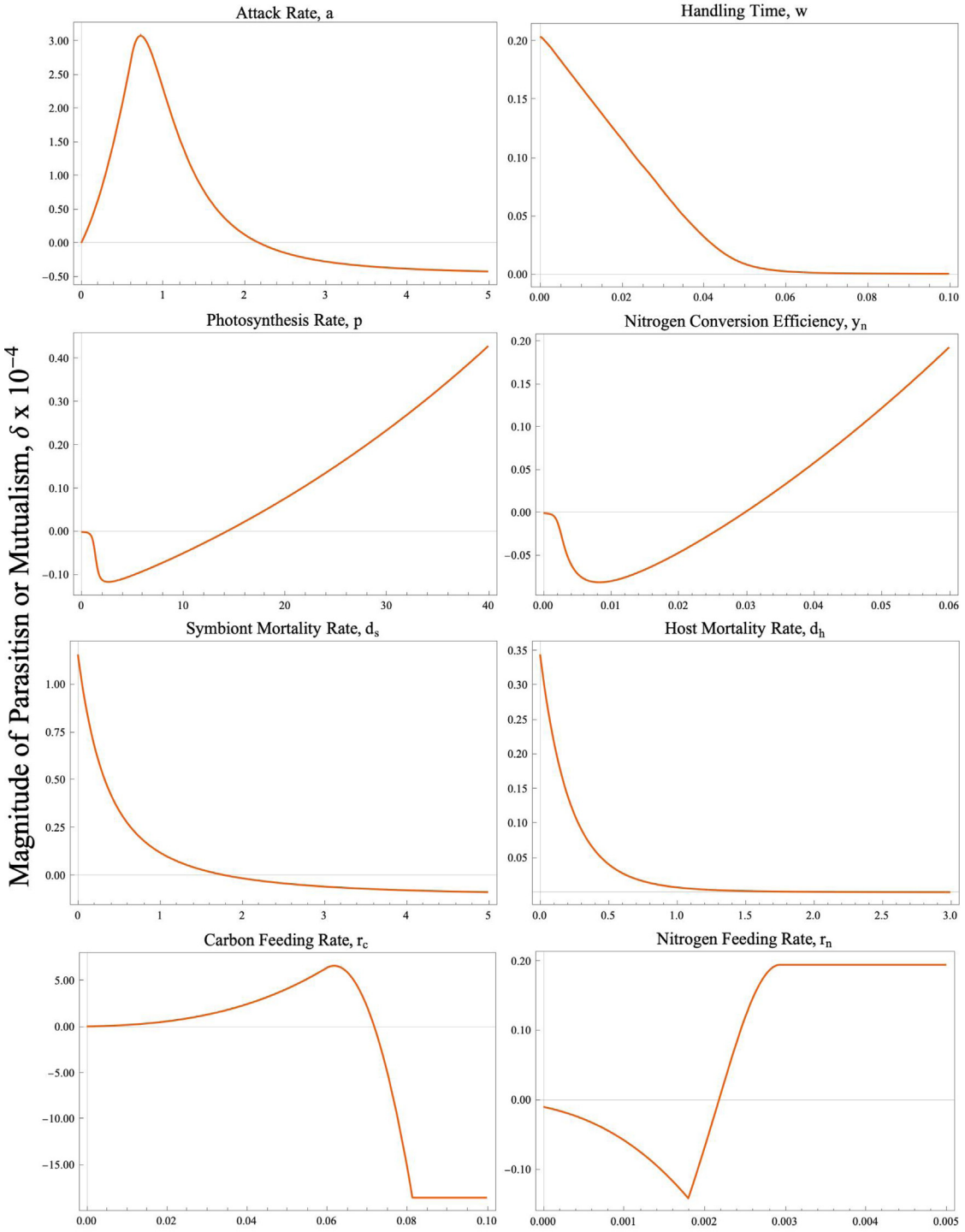

Fig. 4. The parameter values' impact on the δ value of the system. The metric δ is the difference between the biomass of an inoculated anemone and an aposymbiotic anemone after 8 weeks. The symbiont is deemed mutualistic when $\delta > 0$ and parasitic when $\delta < 0$. Each parameter is varied individually, while the other values are kept constant at the fitted values for symbiotic fed anemones. Note that the y-axis is scaled by 10^{-4}.

the symbiont might get nitrogen partially from waste products from the host (Cui et al., 2019; Rahav et al., 1989) or directly from the water column (Cook and D'elia, 1987; Smith and Muscatine, 1999; Davy et al., 2006, 2012) or from particulate organic nitrogen (Davy et al., 2006, 2012). Increased nitrogen availability increases the symbionts' growth eventually leading to significant cost of symbionts on the host and in coral systems, coral bleaching (Wooldridge, 2009). Relaxing the assumption that symbionts can only acquire nitrogen from the host may improve the model's ability to capture the costs of significantly increased growth of the symbiont in higher nitrogen conditions. Similarly, the death rate of the symbiont is a simplification of the death rate of the symbiont and expulsion rate of the symbiont. Though this simplification appears to be appropriate here, it may be less appropriate when the symbionts are limited by light (Jinkerson et al., 2022) or

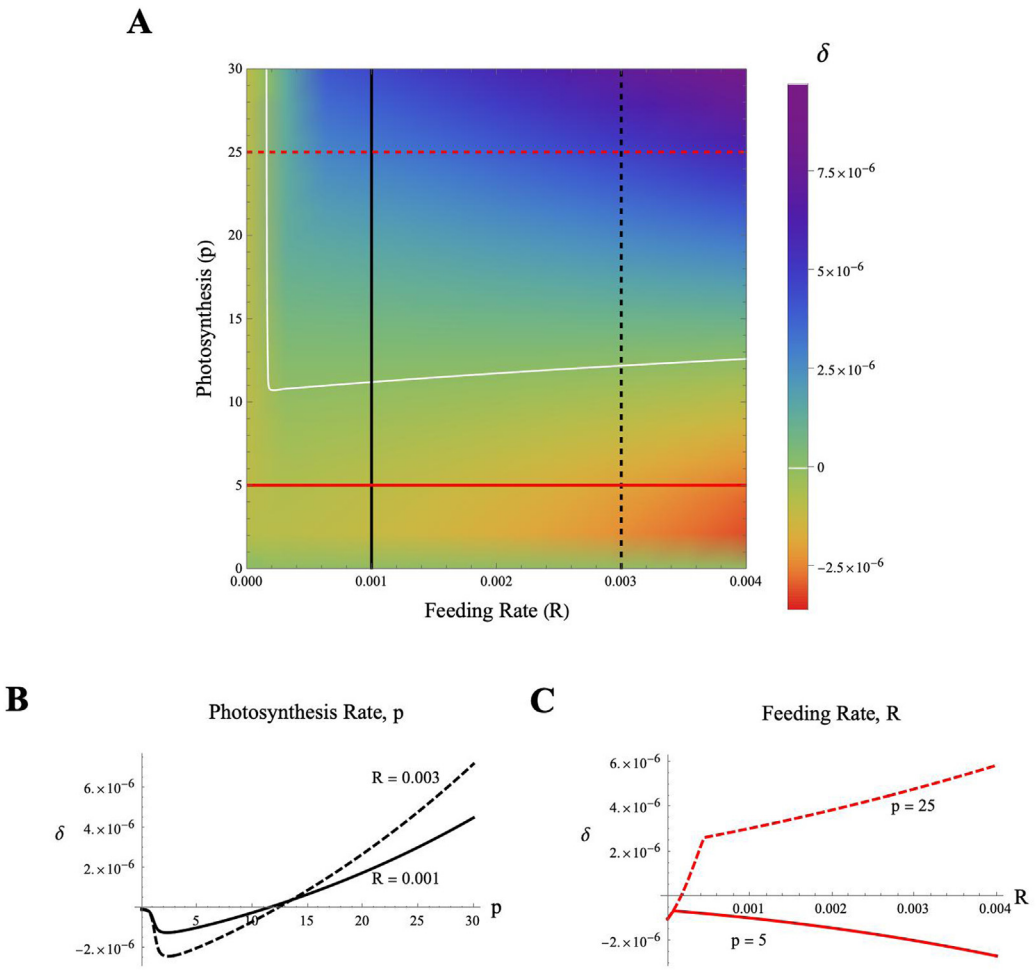

Fig. 5. Plot A: δ as a function of photosynthesis rate of the symbiont (p) and combined uptake rate of the anemone host (R). The metric δ is the difference between the biomass of an inoculated anemone and an aposymbiotic anemone after 8 weeks. The symbiont is deemed mutualistic when $\delta > 0$ and parasitic when $\delta < 0$. The white line represents $\delta = 0$. The black and red lines correspond with those in plots B and C. Plot B: δ as a function of photosynthesis rate (p) at two fixed combined uptake rates ($R = 0.003$ and $R = 0.001$). Plot C: δ as a function of combined uptake rate (R) at two fixed photosynthesis rates ($p = 5$ and $p = 25$).

space (Jones and Yellowlees, 1997). Indeed, there are a variety of ways that Cnidarian hosts may regulate symbiont populations, including limiting nutrient transport to the symbiont and limiting light availability to the symbiont (Baird et al., 2009; Cunning et al., 2015), which are not incorporated into this model. These simplifications limited the number of parameters needed to capture the food dependent symbioses in this system. As our understanding of the exact cost of symbiont on the host, and the molecular pathways that are involved in reverse translocation improves, the model can be adjusted to more accurately capture the molecular dynamics.

Though the set of parameters explored here are specific to *E. pallida* and *B. minutum*, this model has the potential to be applied to other cnidarian-dinoflagellate symbioses. Different symbiont species have varying ability to infect hosts (Dunn and Weis, 2009) and once infected, can have significant varied impacts on the host (Sproles et al., 2020; Cantin et al., 2009; Little et al., 2004; Starzak et al., 2014). Adjusting parameters like the attack rate of the symbiont on the host and nitrogen conversion efficiency (y_n) allows the model to both adjust the cost of the symbiont on the host, and the ability of the symbiont to benefit from changes in the cost. Further, the symbiont does not receive carbon from its host in our model. This has been demonstrated for our host species *E. pallida*, but other species such as *Acropora tenuis* are known to share carbon with their symbionts (Jinkerson et al., 2022). Further adjustments of this model are necessary to capture these differences between species.

This model has clearly demonstrated that the approximation of the symbiont consuming the host can mechanistically describe the system. This model adds to the existing DEB models that describe Cnidarian symbiosis, and reveals the importance of including a direct cost of hosting a symbiont. Furthermore, this work reinforces the need for more experimental evidence to support the exact cellular mechanism that results in reverse translocation and the costs symbionts have on Cnidarian hosts.

CRediT authorship contribution statement

Jakob O. Kaare-Rasmussen: Conceptualization, Methodology, Writing, Visualization. **Holly V. Moeller:** Conceptualization, Methodology, Writing, Visualization. **Ferdinand Pfab:** Conceptualization, Methodology, Writing, Visualization.

Declaration of competing interest

The authors declare that they have no known competing financial interests or personal relationships that could have appeared to influence the work reported in this paper.

Data availability

The code for this project has been implemented in Wolfram Mathematica 13.2. The code is freely available at https://doi.org/10.5281/zenodo.7699157.

Acknowledgments

The authors acknowledge helpful discussion from Roger M. Nisbet and the E5 Coral Epigenetics Modeling Team that aided in formulating this model. The model was illustrated by Elise Cypher.

Funding

This work was supported by the National Science Foundation through research grants EF-1921356 (to HVM). Support was also provided by a Simons Foundation Early Career Award in Marine Microbial Ecology and Evolution (Award # 689265 to HVM).

Appendix A. Anemone and symbiont biomass conversion

In the data from Peng et al. (2020), the anemone were measured in foot base area (mm^2) and the symbionts were measured as the number of symbionts per host. In order to use the data provided by Peng et al. (2020) to parameterize this model, we first need to convert from units of mm^2 and number of symbiont cells to mol C host (H) and mol C symbiont (S). Using the total carbon per symbiont of *B. minutum* sp. found by Wong et al. (2021) we can convert the number of symbiont cells to total *mol C* of symbiont:

$$S = number\ of\ symbiont\ cells \cdot 63\ \frac{\text{pg C}}{cell} \cdot 10^{-12}\ \frac{\text{g}}{\text{pg}} \cdot 12.01^{-1}\ \frac{\text{mol}^{-1}\ \text{C}}{\text{g}} \quad (17)$$

Next, the anemones had two separate morphological forms through the experiment. During the first three weeks all anemone maintained the morphology of a typical anemone, but from the fourth week on some anemones in the symbiotic starved treatments morphologically changed into tissue balls. Due to the morphological differences between an anemone and a tissue ball, we converted from base area to mol C in two distinct ways.

We converted the anemones with typical morphology to C-moles by first calculating base diameter (mm) assuming the base area (mm^2) of an anemone was circular:

$$base\ area = \pi\ (radius)^2 \quad (18)$$

$$radius = \sqrt{\frac{base\ area}{\pi}} \quad (19)$$

$$diameter = 2\sqrt{\frac{base\ area}{\pi}} \quad (20)$$

We then converted diameter (mm) to dry weight (mg) using the conversation found in Leal et al. (2012):

$$dry\ weight = 10^{-0.7013}\ \frac{\text{mg}}{\text{mm}^{2.4124}}(diameter)^{2.4124} \quad (21)$$

Next, since anemone dry weight is approximately 55% carbon, we converted from total mg dry weight to total mg carbon (Zamer, 1986). Finally, we converted mg carbon to g carbon and then g carbon to carbon moles using the molar mass of carbon.

$$H = dry\ weight \cdot 0.55\frac{\text{mg C}}{total\ \text{mg}} \cdot 10^{-3}\ \frac{\text{g}}{\text{mg}} \cdot 12.01^{-1}\ \frac{\text{mol C}}{\text{g}} \quad (22)$$

The final equation to convert an anemone with an anemone morphology is

$$H = 10^{-0.7013} \cdot (2\sqrt{\frac{base\ area}{\pi}})^{2.4124} \cdot 0.55\frac{\text{mg C}}{total\ \text{mg}} \cdot 10^{-3}\ \frac{\text{g}}{\text{mg}} \cdot 12.01^{-1}\ \frac{\text{mol C}}{\text{g}} \quad (23)$$

For the anemone that were described as tissue balls, we assumed the tissue balls were approximately hemispheres as they were still attached to the base of the tank and therefore not full spheres. We assumed the base area of a tissue ball were circular, and calculated the radius (mm) from the base area (mm^2) measurements provided by Peng et al. (2020):

$$base\ area = \pi\ (radius)^2 \quad (24)$$

$$radius = \sqrt{\frac{base\ area}{\pi}} \quad (25)$$

We then used the radius to calculate the volume (mm^3) of tissue balls:

$$volume = \frac{2}{3}\pi(radius)^3 \quad (26)$$

We assumed that the wet weight (mg) of an anemone tissue ball was approximately the weight of an equivalent volume of water. Using the results of, Leal et al. (2012) (Fig. 1.A) we found that anemone dry weight (mg) is approximately 0.16 of the wet weight (mg).

$$dry\ weight = volume \cdot \frac{1\ \text{mg}}{1\ \text{mm}^3} \cdot 0.16\frac{\text{mg}}{\text{mg}} \quad (27)$$

Next, anemone dry weight is approximately 55% carbon and we converted mg carbon to g carbon and use the molar mass of carbon to convert to mol C (Zamer, 1986). The final equation to convert base area of tissue balls is

$$H = \frac{2}{3}\pi(radius)^3 \cdot 0.16\ \frac{\text{mg}}{\text{mg}} \cdot 0.55\frac{\text{mg C}}{total\ \text{mg}} \cdot 10^{-3}\ \frac{\text{g}}{\text{mg}} \cdot 12.01^{-1}\ \frac{\text{mol C}}{\text{g}} \quad (28)$$

Peng et al. (2020) provided the number of anemones that had become tissue balls each week for each treatment, but did not specify exactly which anemone changed to tissue balls. For weeks with tissue balls, we transformed the smallest base area measurements to tissue balls. For example, on week 4 of the starved symbiotic anemone treatment there was only one anemone that had become a tissue ball, so we transformed the smallest base area as a tissue ball, and all the others as anemone with anemone morphology.

Appendix B. Parameter fitting

This model was built to understand the dynamics of the anemone and symbiont system under four separate treatments and six distinct data sets provided by Peng et al. (2020). There are four anemone data sets of the base area of the anemone corresponding to all four treatments. There are two symbiont data sets of the number of symbionts per anemone corresponding to the two inoculated treatments. All parameters except S_0, r_n and r_c are fit to one value throughout all treatments. The parameter y_c is set to be zero assuming that the symbiont gains no carbohydrates from the host. The parameters S_0, r_n and r_c correspond to presence or absence of feeding and the presence or absences of the symbiont, and are therefore not the same in all treatments. The parameters are either set to zero or adopt each their own fitted value. Note that these parameters are only fitted to one value, not to separate values for each non-zero treatment. For example, the parameter S_0 is set to zero for all aposymbiotic treatments, but is fit to one value for both the inoculated treatments.

To parameterize this model, we used the method outlined in Jager and Ashauer (2018). We calculate the minimum log-likelihood, ℓ_i, for each data set, i as:

$$\ell_i = c - \frac{\lambda_i}{2}\log(s_i) \quad (29)$$

where λ_i is the number of data points in the data set i and c is a constant. The constant only depends on the data and not on the dimensions, and therefore can be dropped in the optimization. s_i is the sum of squared error of variables x ($x = H$ for anemone data sets and $x = S$ for symbiont data sets):

$$s_i = \sum_j (\tilde{x}(t_j) - x_j)^2 \quad (30)$$

where $\tilde{x}(t_j)$ is the model prediction at time t_j and x_j is the actual value at time t_j. The joint log likelihood for all data sets is the sum of each individual ℓ_i:

$$\ell_{total} = \sum_{i=1}^{6} \ell_i \quad (31)$$

This follows from the assumption that the standard deviations are different between data-sets. Minimizing ℓ_{total} for some set of parameters provided us with parameter values that maximized the fit for all treatments. The fitted parameter values can be found in Table 2.

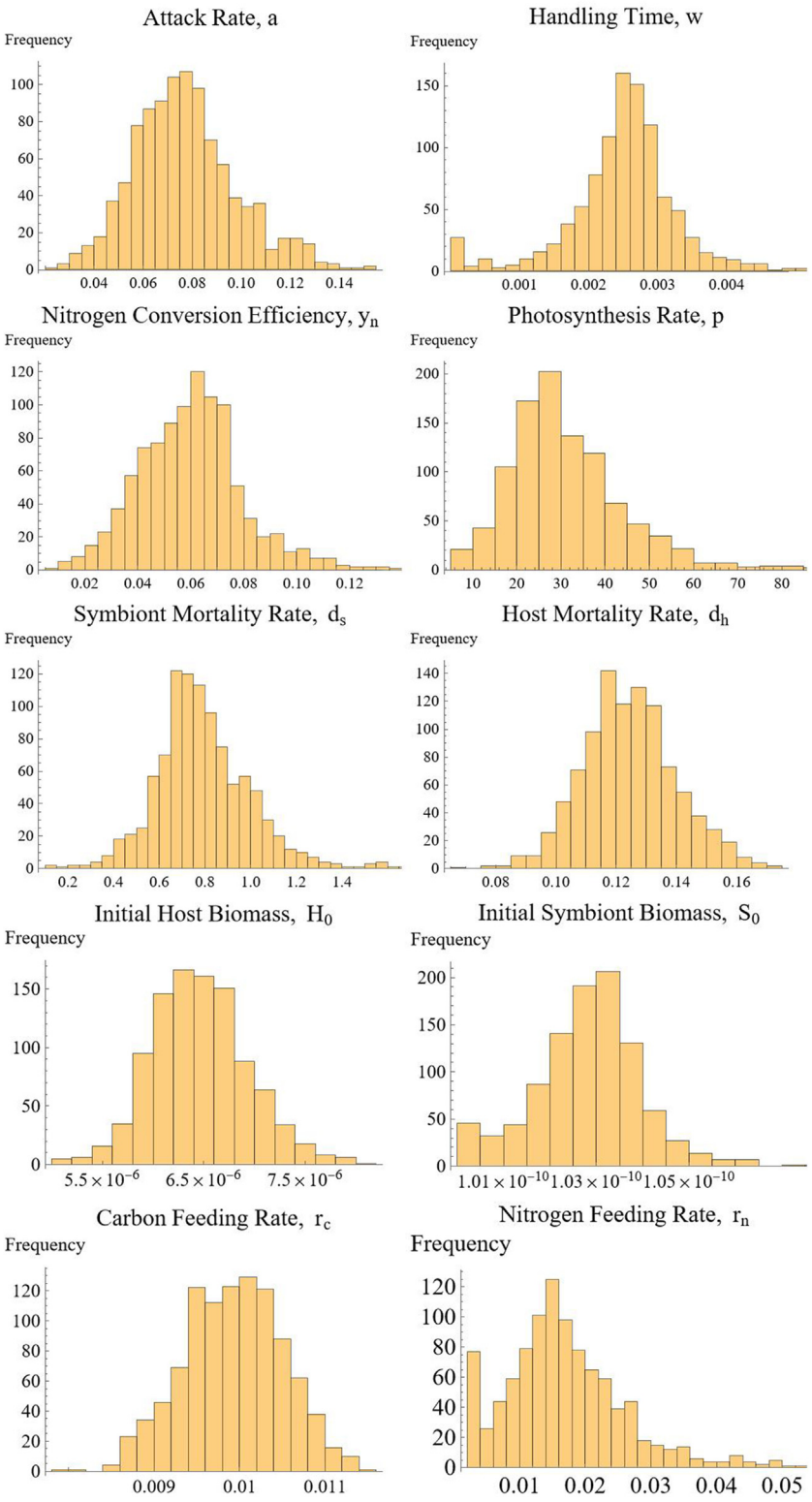

Fig. 6. Distribution of bootstrapped parameter values for all fitted parameters. These distributions are used to find the 95% confidence intervals of the parameter values using the Bias-Corrected and Accelerated (BC_a) method outlined by Efron and Tibshirani (1994). The parameter values and 95% confidence intervals can be found in Table 2.

Appendix C. Bootstrapping distributions and confidence intervals

Since we had 420 distinct data points to fit this model to, we found bootstrapping, as described in Efron and Tibshirani (1994), to be an appropriate method to estimate 95% confidence intervals for the fitted parameter values. We sampled each of the six data sets λ_i times with replacement where λ_i represents the number of data points in the data set i. After sampling all six of the data sets, we refitted the model. We completed this process 1000 times, re-sampling the data and fitting the model each time. This process providing us with a distribution of parameter values for each parameter as shown in Appendix Fig. 6. Most of the distributions were non-normal, so simple methods, like reverse

percentile interval, could not be used to extract the 95% confidence intervals from the distribution. Instead, to account for the non-normal distributions, we used the *Bias-Corrected and Accelerated* (BC_a) method as described in Efron and Tibshirani (1994) Chapter 14 to extract the 95% confidence intervals, which are shown in Table 2.

Appendix D. Supplementary data

Supplementary material related to this article can be found online at https://doi.org/10.1016/j.ecolmodel.2023.110325. The Supplementary Materials contain further analysis of the dynamics of nutrient limitations in this model.

References

Baird, Andrew H., Bhagooli, Ranjeet, Ralph, Peter J., Takahashi, Shunichi, 2009. Coral bleaching: the role of the host. Trends Ecol. Evol. 24 (1), 16–20.

Baker, David M., Freeman, Christopher J., Wong, Jane C.Y., Fogel, Marilyn L., Knowlton, Nancy, 2018. Climate change promotes parasitism in a coral symbiosis. ISME J. 12 (3), 921–930.

Banaszak, Anastazia T., Ramos, Maribel García, Goulet, Tamar L., 2013. The symbiosis between the gastropod *Strombus gigas* and the dinoflagellate *Symbiodinium*: an ontogenic journey from mutualism to parasitism. J. Exp. Mar. Biol. Ecol. 449, 358–365.

Cantin, Neal E., van Oppen, Madeleine J.H., Willis, Bette L., Mieog, Jos C., Negri, Andrew P., 2009. Juvenile corals can acquire more carbon from high-performance algal symbionts. Coral Reefs 28 (2), 405–414.

Clayton, Jr., William S., Lasker, Howard R., 1984. Host feeding regime and zooxanthellal photosynthesis in the anemone, *Aiptasia pallida* (Verrill). Biol. Bull. 167 (3), 590–600.

Cook, Clayton B., 1972. Benefit to symbiotic zoochlorellae from feeding by green hydra. Biol. Bull. 142 (2), 236–242.

Cook, Clayton B., D'elia, Christopher F., 1987. Review article are natural populations of zooxanthellae ever nutrient-limited? Symbiosis.

Cornwall, Andrew, 2017. The Importance and Movement of Mud Bacterial Carbon Within the Symbiosis of the New Zealand Sea Anemone *Anthopleura Aureoradiata*. Victoria University of Wellington.

Crossland, C.J., Hatcher, B.G., Smith, S.V., 1991. Role of coral reefs in global ocean production. Coral Reefs 10 (2), 55–64.

Cui, Guoxin, Liew, Yi Jin, Li, Yong, Kharbatia, Najeh, Zahran, Noura I., Emwas, Abdul-Hamid, Eguiluz, Victor M., Aranda, Manuel, 2019. Host-dependent nitrogen recycling as a mechanism of symbiont control in *Aiptasia*. PLoS Genet. 15 (6), e1008189.

Cunning, Ross, Muller, Erik B., Gates, Ruth D., Nisbet, Roger M., 2017. A dynamic bioenergetic model for coral-Symbiodinium symbioses and coral bleaching as an alternate stable state. J. Theoret. Biol. 431, 49–62.

Cunning, Ross, Vaughan, Nathan, Gillette, Phillip, Capo, Tom R., Mate, J.L., Baker, Andrew C., 2015. Dynamic regulation of partner abundance mediates response of reef coral symbioses to environmental change. Ecology 96 (5), 1411–1420.

Davy, Simon K., Allemand, Denis, Weis, Virginia M., 2012. Cell biology of cnidarian-dinoflagellate symbiosis. Microbiol. Mol. Biol. Rev. 76 (2), 229–261.

Davy, Simon K., Cook, Clayton B., 2001. The influence of 'host release factor'on carbon release by zooxanthellae isolated from fed and starved *Aiptasia pallida* (Verrill). Comp. Biochem. Physiol A Mol. Integr. Physiol. 129 (2–3), 487–494.

Davy, Simon K., Withers, Karen J.T., Hinde, Rosalind, 2006. Effects of host nutritional status and seasonality on the nitrogen status of zooxanthellae in the temperate coral *Plesiastrea versipora* (Lamarck). J. Exp. Mar. Biol. Ecol. 335 (2), 256–265.

Dunn, Simon R., Weis, Virginia M., 2009. Apoptosis as a post-phagocytic winnowing mechanism in a coral–dinoflagellate mutualism. Environ. Microbiol. 11 (1), 268–276.

Efron, Bradley, Tibshirani, Robert J., 1994. An Introduction to the Bootstrap. CRC Press.

Falkowski, Paul G., Dubinsky, Zvy, Muscatine, Leonard, Porter, James W., 1984. Light and the bioenergetics of a symbiotic coral. Bioscience 34 (11), 705–709.

Falkowski, Paul G., Raven, John A., 2013. Aquatic Photosynthesis. Princeton University Press.

Fang, James K.H., Schönberg, Christine H.L., Hoegh-Guldberg, Ove, Dove, Sophie, 2017. Symbiotic plasticity of *Symbiodinium* in a common excavating sponge. Mar. Biol. 164 (5), 1–11.

Farrant, P.A., Borowitzka, M.A., Hinde, R., King, R.J., 1987. Nutrition of the temperate Australian soft coral *Capnella gaboensis*. Mar. Biol. 95 (4), 565–574.

Fisher, Rebecca, O'Leary, Rebecca A., Low-Choy, Samantha, Mengersen, Kerrie, Knowlton, Nancy, Brainard, Russell E., Caley, M. Julian, 2015. Species richness on coral reefs and the pursuit of convergent global estimates. Curr. Biol. 25 (4), 500–505.

Grant, A.J., Rémond, M., Starke-Peterkovic, T., Hinde, R., 2006. A cell signal from the coral *Plesiastrea versipora* reduces starch synthesis in its symbiotic alga, *Symbiodinium* sp. Comp. Biochem. Physiol A Mol. Integr. Physiol. 144 (4), 458–463.

Holling, Crawford S., 1959. Some characteristics of simple types of predation and parasitism. Can. Entomol. 91 (7), 385–398.

Hughes, Terry P., Anderson, Kristen D., Connolly, Sean R., Heron, Scott F., Kerry, James T., Lough, Janice M., Baird, Andrew H., Baum, Julia K., Berumen, Michael L., Bridge, Tom C., et al., 2018. Spatial and temporal patterns of mass bleaching of corals in the anthropocene. Science 359 (6371), 80–83.

Jager, Tjalling, Ashauer, Roman, 2018. Modelling Survival Under Chemical Stress: a Comprehensive Guide to the GUTS Framework. ISBN: 978-1-9999705-0-5.

Jeong, Hae Jin, Du Yoo, Yeong, Kang, Nam Seon, Lim, An Suk, Seong, Kyeong A.h., Lee, Sung Yeon, Lee, Moo Joon, Lee, Kyung Ha, Kim, Hyung Seop, Shin, Woongghi, et al., 2012. Heterotrophic feeding as a newly identified survival strategy of the dinoflagellate *Symbiodinium*. Proc. Natl. Acad. Sci. 109 (31), 12604–12609.

Jinkerson, Robert E., Russo, Joseph A., Newkirk, Casandra R., Kirk, Andrea L., Chi, Richard J., Martindale, Mark Q., Grossman, Arthur R., Hatta, Masayuki, Xiang, Tingting, 2022. Cnidarian-symbiodiniaceae symbiosis establishment is independent of photosynthesis. Curr. Biol.

Jones, Ross J., Yellowlees, D., 1997. Regulation and control of intracellular algae (=zooxanthellae) in hard corals. Philos. Trans. R. Soc. London [Biol.] 352 (1352), 457–468.

Kooijman, S.A.L.M, 2001. Quantitative aspects of metabolic organization: a discussion of concepts. Philos. Trans. R. Soc. London [Biol.] 356 (1407), 331–349.

Leal, Miguel Costa, Nunes, Cristóvão, Engrola, Sofia, Dinis, Maria Teresa, Calado, Ricardo, 2012. Optimization of monoclonal production of the glass anemone *Aiptasia pallida* (Agassiz in Verrill, 1864). Aquaculture 354, 91–96.

Lesser, M.P., Stat, Michael, Gates, R.D., 2013. The endosymbiotic dinoflagellates (*Symbiodinium* sp.) of corals are parasites and mutualists. Coral Reefs 32 (3), 603–611.

Little, Angela F., Van Oppen, Madeleine J.H., Willis, Bette L., 2004. Flexibility in algal endosymbioses shapes growth in reef corals. Science 304 (5676), 1492–1494.

Morris, Luke A., Voolstra, Christian R., Quigley, Kate M., Bourne, David G., Bay, Line K., 2019. Nutrient availability and metabolism affect the stability of coral–Symbiodiniaceae symbioses. TIM 27 (8), 678–689.

Muller, Erik B., Kooijman, Sebastiaan A.L.M, Edmunds, Peter J., Doyle, Francis J., Nisbet, Roger M., 2009. Dynamic energy budgets in syntrophic symbiotic relationships between heterotrophic hosts and photoautotrophic symbionts. J. Theoret. Biol. 259 (1), 44–57.

Muscatine, Leonard, Cernichiari, Elsa, 1969. Assimilation of photosynthetic products of zooxanthellae by a reef coral. Biol. Bull. 137 (3), 506–523.

Muscatine, Leonard, Porter, James W., 1977. Reef corals: mutualistic symbioses adapted to nutrient-poor environments. Bioscience 27 (7), 454–460.

Nisbet, R.M., Muller, E.B., Lika, K., Kooijman, S.A.L.M, 2000. From molecules to ecosystems through dynamic energy budget models. J. Anim. Ecol. 913–926.

Peng, Shao-En, Moret, Alessandro, Chang, Cherilyn, Mayfield, Anderson B., Ren, Yu-Ting, Chen, Wan-Nan U., Giordano, Mario, Chen, Chii-Shiarng, 2020. A shift away from mutualism under food-deprived conditions in an anemone-dinoflagellate association. PeerJ 8, e9745.

Rädecker, Nils, Raina, Jean-Baptiste, Pernice, Mathieu, Perna, Gabriela, Guagliardo, Paul, Kilburn, Matt R., Aranda, Manuel, Voolstra, Christian R., 2018. Using *Aiptasia* as a model to study metabolic interactions in cnidarian-*Symbiodinium* symbioses. Front. Physiol. 9, 214.

Rahav, O., Dubinsky, Z., Achituv, Y., Falkowski, P.G., 1989. Ammonium metabolism in the zooxanthellate coral, stylophora pistillata. Philos. Trans. R. Soc. London [Biol.] 236 (1284), 325–337.

Russo, Sabrina E., Ledder, Glenn, Muller, Erik B., Nisbet, Roger M., 2022. Dynamic Energy Budget models: fertile ground for understanding resource allocation in plants in a changing world. Conserv. Physiol. 10 (1), coac061.

Sachs, Joel L., Wilcox, Thomas P., 2006. A shift to parasitism in the jellyfish symbiont *Symbiodinium microadriaticum*. Phil. Trans. R. Soc. B 273 (1585), 425–429.

Siegel, R.W., 1960. Hereditary endosymbiosis in paramecium bursaria. Exp. Cell Res. 19 (2), 239–252.

Smith, G.J., Muscatine, L., 1999. Cell cycle of symbiotic dinoflagellates: variation in G1 phase-duration with anemone nutritional status and macronutrient supply in the *Aiptasia pulchella–Symbiodinium pulchrorum* symbiosis. Mar. Biol. 134 (3), 405–418.

Sproles, Ashley E., Oakley, Clinton A., Krueger, Thomas, Grossman, Arthur R., Weis, Virginia M., Meibom, Anders, Davy, Simon K., 2020. Sub-cellular imaging shows reduced photosynthetic carbon and increased nitrogen assimilation by the non-native endosymbiont durusdinium trenchii in the model cnidarian aiptasia. Environ. Microbiol. 22 (9), 3741–3753.

Starzak, Dorota E., Quinnell, Rosanne G., Nitschke, Matthew R., Davy, Simon K., 2014. The influence of symbiont type on photosynthetic carbon flux in a model cnidarian–dinoflagellate symbiosis. Mar. Biol. 161 (3), 711–724.

Stat, Michael, Morris, Emily, Gates, Ruth D., 2008. Functional diversity in coral–dinoflagellate symbiosis. Proc. Natl. Acad. Sci. 105 (27), 9256–9261.

Steen, R. Grant, 1986. Evidence for heterotrophy by zooxanthellae in symbiosis with *Aiptasia pulchella*. Biol. Bull. 170 (2), 267–278.

Steen, R.G., 1987. Evidence for facultative heterotrophy in cultured zooxanthellae. Mar. Biol. 95 (1), 15–23.

Steen, R. Grant, 1988. The bioenergetics of symbiotic sea anemones (Anthozoa: Actiniaria). Symbiosis 5 (1–2), 103–142.

Tremblay, Pascale, Gori, Andrea, Maguer, Jean François, Hoogenboom, Mia, Ferrier-Pagès, Christine, 2016. Heterotrophy promotes the re-establishment of photosynthate translocation in a symbiotic coral after heat stress. Sci. Rep. 6 (1), 1–14.

van der Meer, Jaap, 2006. An introduction to Dynamic Energy Budget (DEB) models with special emphasis on parameter estimation. J. Sea Res. 56 (2), 85–102.

Van Oppen, Madeleine J.H., Lough, Janice M., 2018. Synthesis: Coral Bleaching: Patterns, Processes, Causes and Consequences. Springer.

von Liebig, Justus, 1841. Die organische Chemie in ihrer Anwendung auf Agricultur und Physiologie. Vieweg.

Wolfram Research, Inc., 2021. Mathematica, Version 13.2.0. URL https://www.wolfram.com/mathematica, Champaign, IL, 2021.

Wong, Jane C.Y., Enríquez, Susana, Baker, David M., 2021. Towards a trait-based understanding of Symbiodiniaceae nutrient acquisition strategies. Coral Reefs 40 (2), 625–639.

Wooldridge, Scott A., 2009. A new conceptual model for the warm-water breakdown of the coral–algae endosymbiosis. Mar. Freshwater Res. 60 (6), 483–496.

Wooldridge, Scott A., 2010. Is the coral-algae symbiosis really 'mutually beneficial'for the partners? BioEssays 32 (7), 615–625.

Xiang, Tingting, Lehnert, Erik, Jinkerson, Robert E., Clowez, Sophie, Kim, Rick G., DeNofrio, Jan C., Pringle, John R., Grossman, Arthur R., 2020. Symbiont population control by host-symbiont metabolic interaction in Symbiodiniaceae-cnidarian associations. Nature Commun. 11 (1), 1–9.

Xu, Yi, Zhang, Jing, Huang, Hui, Yuan, Xiangcheng, Zhang, Junxiao, Ge, Jianzhong, 2022. Coral symbiosis carbon flow: A numerical model study spanning cellular to ecosystem levels. Front. Mar. Sci. (ISSN: 2296-7745) 9, http://dx.doi.org/10.3389/fmars.2022.749921, URL https://www.frontiersin.org/article/10.3389/fmars.2022.749921.

Zamer, W.E., 1986. Physiological energetics of the intertidal sea anemone Anthopleura elegantissima. Mar. Biol. 92 (3), 299–314.